

MAGNETOINTERBAND CONTRIBUTION TO THIRD-HARMONIC
GENERATION IN InSb USING A CO₂ LASER

N. Van Tran, J. H. McFee, and C. K. N. Patel
Bell Telephone Laboratories, Holmdel, New Jersey
(Received 8 July 1968)

Enhancement of the third-harmonic generation has been observed in InSb in the presence of a magnetic field. The magnetic field values corresponding to maximum third-harmonic generation are found to be 7% lower than those corresponding to the interband magnetoabsorption resonances in InSb.

The 10.6- μ radiation from the CO₂ laser provides a powerful tool for studying multiphoton plasma production,¹ multiphoton magnetoabsorption,² and frequency mixing^{3,4} in narrow-gap semiconductors. Recently, Lax, Zawadzki, and Weiler⁵ have pointed out the possibility of enhancement in third-harmonic generation (THG) due to interband transitions in the presence of a magnetic field. Using a semiclassical treatment for bound oscillators in a two-band nonparabolic model, Lax, Zawadzki, and Weiler⁵ show that the enhancement of THG occurs when

$$3\hbar\omega = [E_g^2 + 4E_g \hbar\omega_c (n + \frac{1}{2})]^{1/2}, \quad (1)$$

where $3\hbar\omega$ is the energy of the TH photon, ω_c the cyclotron frequency of an electron at the bottom of the conduction band, E_g the band gap, and n the quantum number of the Landau levels. Figure 1 represents schematically the resonant condition stated in Eq. (1). Maximum enhancement occurs when $3\hbar\omega$ is equal to the energy separation between a Landau level in the conduction band and a Landau level in the valence band.⁶

In this paper we report the observation of THG enhancement in InSb in the presence of a magnetic field. A fundamental power of 1- to 5-kW peak (250-nsec pulse width and 120-cps repetition rate) at $\lambda = 10.6 \mu$ was obtained from a Q-switched CO₂ laser. A gated integrator was used to average the TH signals over times of the order of 10 sec. The InSb single-crystal samples were in the form of thin plates having dimensions $4 \times 4 \times \sim 0.0015 \text{ mm}^3$, and were maintained at 15°K. A magnetic field of 0-54 kOe was provided by a superconducting solenoid. The field of this solenoid was precisely proportional to the current, and no hysteresis effect was observed. The magnetic field and the propagation vector of the incident radiation were along the thin dimension of the sample, which was chosen to be either the $\langle 110 \rangle$ or $\langle 100 \rangle$ crystallographic direction. When the incident radiation was linearly polarized, its electric field was made parallel to $\langle 100 \rangle$ in order

to suppress the third harmonic produced by mixing of the second harmonic with the fundamental. The electron concentration of our samples was approximately 10^{14} cm^{-3} and the electron mobility was $6 \times 10^5 \text{ cm}^2/\text{V sec}$ at 77°K.

In Figs. 2(a) and 2(b) we show for InSb the TH power ($\lambda = 3.53 \mu$) as a function of the applied magnetic field for $B \parallel \langle 110 \rangle$ and $B \parallel \langle 100 \rangle$, respectively. At least seven peaks in the THG can be seen in the range 0-54 kOe.⁷ The observed B values corresponding to the maxima of THG for InSb sample A are given in column 1 of Table I. To obtain these data, the magnetic field was swept at a constant rate. Therefore, because of the 10-sec effective time constant of the signal integrator, the positions of the THG peaks are shifted slightly to the right for increasing B (as in Fig. 2) or slightly to the left for decreasing B . Each of our B values in Table I is the average of the values found for the two directions of field

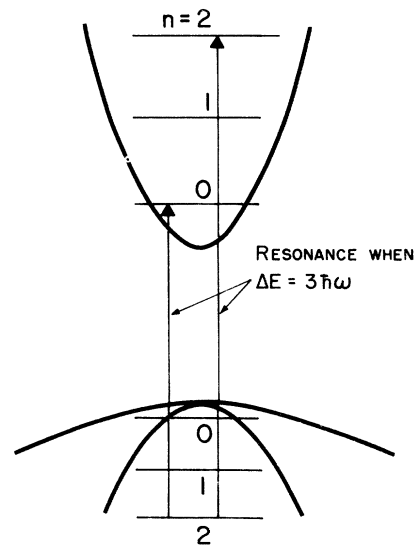


FIG. 1. Schematic representation of energy levels in InSb in the presence of a magnetic field. Arrows indicate allowed interband transitions between Landau levels in the light-hole valence band and the conduction band.

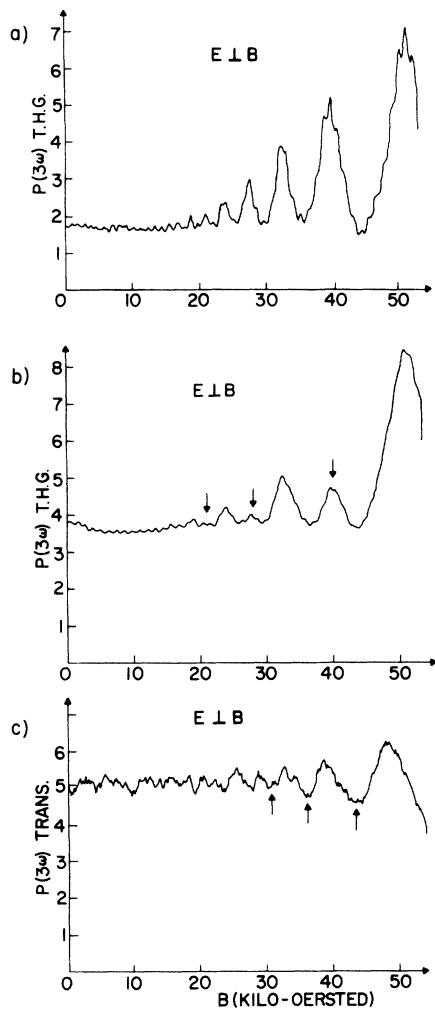


FIG. 2. (a), (b) Typical dependence of third-harmonic power generated in InSb at 15°K on applied magnetic field. Magnetic field parallel to $\langle 110 \rangle$ in (a) and parallel to $\langle 100 \rangle$ in (b). In (b) arrows indicate suppressed peaks. (c) Observed dependence of transmission of third-harmonic signal generated external to InSb sample on magnetic field (parallel to $\langle 110 \rangle$). (Arrows indicate positions of minima in transmission.)

sweep. These values of B were independent of the intensity of the 10.6- μ radiation. It is interesting to compare these results with the comprehensive magnetointerband absorption study made on InSb by Pidgeon and Brown.⁸ In their experiments, the photon whose energy is equal to the separation between a Landau level in the conduction band and a Landau level in the valence band is strongly absorbed. For comparison with our results we use the data shown by Pidgeon and Brown in Fig. 1 of Ref. 8, which gives the transmission minima as a function of magnetic field for the allowed transitions between the light-hole

valence band and the conduction band. The values of magnetic field corresponding to the transmission minima for the photon at $\lambda = 3.53 \mu$ ($3\hbar\omega = 0.351 \text{ eV}$) are given in column 2 of Table I. The transition identification numbers and the change in magnetic quantum number (Δn) values assigned to each minimum by Pidgeon and Brown are shown in column 3 of Table I. If, as in Table I, we make the assignment that our THG peak at 51.6 kG corresponds to Pidgeon and Brown's transition No. 5, we find that all of our THG maxima occur at B values which are about 6% lower than the B values at which Pidgeon and Brown observe minimum transmission (see column 4 of Table I). Further experimental support for this assignment is provided by THG measurements made using the 9.6- μ output from the CO₂ laser as the fundamental. In this case, using the transition identification established from the 10.6- μ measurements, we find the same constant percent discrepancy between the THG maxima and the Pidgeon and Brown data.

We also call attention to the amplitude of the peak in the TH power as a function of the magnetic field. Figure 2(a) shows a monotonic increase in the amplitude of the successive peaks as the magnetic field is increased parallel to the $\langle 110 \rangle$ direction. When the magnetic field is parallel to $\langle 100 \rangle$, the THG maxima occur at the same values of B as in Fig. 2(a); but we observe a suppression of the peaks corresponding to $\Delta n = 0$ [see Fig. 2(b) and column 3 of Table I]. We have looked for a correlation between the behavior of the THG amplitude and the magnetoabsorption by making measurements on both $\langle 110 \rangle$ and $\langle 100 \rangle$ samples using the 3.508- μ output of a He-Xe laser as a source. In contrast to the THG data, the 3.508- μ results do not show the alteration of intensities observed in the THG data when $\langle 100 \rangle$ is parallel to \vec{B} . Therefore, the causes underlying this feature of the THG results are not at present understood.

The experimental conditions under which the data of Pidgeon and Brown shown in Table I were obtained appear to approximate closely the conditions of our THG experiments. However, such factors as a discrepancy in the magnetic field calibration or the presence of strain in the sample⁹ could make the comparison of our THG results with the magnetoabsorption data of Pidgeon and Brown quite meaningless. In order to check on such a possibility, we have measured the transmission of our samples using a TH signal ($\lambda = 3.53 \mu$) generated external to the InSb sam-

Table I. Comparison of THG and magnetoabsorption data.

(1)	(2)	(3)		(4)	(5)	(6)
THG maxima for sample A ^a	Transmission minima for $\lambda = 3.53 \mu^b$	Transition		Percent discrepancy	Transmission minima for sample A ^d	Percent discrepancy
(kOe)	(kOe)	No. ^c	Δn^c	$\frac{(2)-(1)}{(2)} \times 100$	(kOe)	$\frac{(5)-(1)}{(5)} \times 100$
51.6	54.8	5	-2	5.5	>53.8 ^e	
39.9	42.0	6	0	5.0	42.8	6.8
32.6	34.8	7	-2	6.3	34.9	6.6
27.4	29.2	8	0	6.2	29.6	7.4
23.6	25.3	9	-2	6.7		
20.8	22.0	10	0	5.8		
18.5	20.0	11	-2	7.5		

^aFundamental wavelength = 10.6 μ . Reproducibility of these measurements is $\pm 1\%$.

^bData taken from Pidgeon and Brown (Ref. 8), Fig. 1.

^cIdentification number of transition and change in magnetic quantum number (Δn) are as defined by Pidgeon and Brown in Fig. 1 of Ref. 8.

^dTransmission data obtained by use of 3.53- μ signal generated external to sample A.

^e53.8 kOe is the highest field obtainable in our experiments.

ple. For this purpose, the signal at 3.53 μ was obtained from an InAs crystal placed in the fundamental beam used in the THG experiments. In this way, our transmission measurements were performed on the same InSb sample under exactly the same experimental conditions as in the THG measurements. Figure 2(c) shows a typical result for our observed 3.53- μ transmission as a function of the magnetic field. In column 5 of Table I we give the observed magnetic field values corresponding to minimum transmission through InSb sample A. These values agree with in experimental error ($\pm 2\%$) with the values of Pidgeon and Brown (column 2). Thus we conclude that the comparison between our THG results and the magnetoabsorption data of Pidgeon and Brown is meaningful, and that the THG peaks occur at values of the magnetic field which are about 7% lower than the field values corresponding to minimum transmission of the TH. (See columns 4 and 6 of Table I.)

The existence of a discrepancy between THG enhancement and the magnetoabsorption resonance is not entirely unexpected. Since the TH photon is strongly absorbed ($\alpha \approx 3 \times 10^4 \text{ cm}^{-1}$), the TH power $P(3\omega)$ is given by^{10,11}

$$P(3\omega) \propto \frac{|\chi_{NL}^{(3\omega)}|^2 E^6}{[\epsilon_L'(3\omega) - \epsilon_L(\omega)]^2 + \epsilon_L''(3\omega)^2}. \quad (2)$$

Here $\chi_{NL}^{(3\omega)}$ is the complex third-order sus-

ceptibility; $\epsilon_L'(3\omega)$ and $\epsilon_L''(3\omega)$ are the real and imaginary parts of the linear dielectric constant at 3ω ; $\epsilon_L(\omega)$ is the linear dielectric constant at ω and is real because the absorption of the sample at 10.6 μ is very small. E is the electric field strength at the fundamental frequency. Since the energy of the photon at the TH frequency is considerably larger (0.35 eV) than the band gap (0.23 eV) and the quantum numbers of the Landau levels involved are high, it follows that $[\epsilon_L'(3\omega) - \epsilon_L(\omega)]^2 \ll \epsilon_L''(3\omega)^2$. Hence

$$P(3\omega) \propto |\chi_{NL}^{(3\omega)}|^2 E^6 / \epsilon_L''(3\omega)^2. \quad (3)$$

Our transmission measurements show that the variation of TH absorption from 0 to 54 kOe is about 10%. In this case, the variation of $\epsilon_L''(3\omega)^2$ is only about 1%. Thus the dispersion of $P(3\omega)$ will be entirely determined by the dispersion of $\chi_{NL}^{(3\omega)}$. It follows that the maximum enhancement of THG will not necessarily occur at the same B value where maximum absorption of 3ω is observed, corresponding to a maximum in the imaginary part of $\epsilon(3\omega)$.

In summary, we have observed enhancement of THG in InSb in the presence of a magnetic field. The detailed behavior of the TH power as a function of magnetic field correlates well, but not exactly, with the interband magnetoabsorption resonances in InSb, as predicted by Lax et al. The observed discrepancy between the mag-

netic field values corresponding to the maxima of THG and those corresponding to the transmission minima requires more theoretical work about the details of nonlinear dispersion at frequencies larger than the band gap.

We would like to thank S. J. Buchsbaum and P. A. Wolff for helpful comments on the manuscript, J. W. Klüver for help in the 3.508- μ transmission measurements, and Victor C. Wade for his skillful preparation of the thin samples.

¹C. K. N. Patel, P. A. Fleury, R. E. Slusher, and H. L. Frisch, *Phys. Rev. Letters* **16**, 971 (1966).

²K. J. Button, Benjamin Lax, Margaret H. Weiler, and M. Reine, *Phys. Rev. Letters* **17**, 1005 (1966).

³C. K. N. Patel, R. E. Slusher, and P. A. Fleury, *Phys. Rev. Letters* **17**, 1011 (1966).

⁴P. A. Wolff and G. A. Pearson, *Phys. Rev. Letters*

17, 1015 (1966).

⁵B. Lax, W. Zawadzki, and M. H. Weiler, *Phys. Rev. Letters* **18**, 462 (1967).

⁶Equation (1) applies only to the case in which the interband transition involves Landau levels having the same quantum number n .

⁷All the data shown in Fig. 2 are obtained using a linearly polarized fundamental beam. We find that there is no observable THG when the fundamental beam is circularly polarized. This result is to be expected if the isotropic model for the band structure is used to calculate the third-order nonlinear susceptibility.

⁸C. R. Pidgeon and R. N. Brown, *Phys. Rev.* **146**, 575 (1966).

⁹G. G. MacFarlane, T. P. McLean, J. E. Quarrington, and V. Roberts, *Phys. Rev. Letters* **2**, 252 (1959).

¹⁰N. Bloembergen and P. S. Pershan, *Phys. Rev.* **128**, 606 (1962).

¹¹R. A. Soref, Stanford Electronics Laboratory, Stanford University, Technical Report No. 0556-8, 1963 (unpublished).

GRAPHITE TRIPLE POINT AND SOLIDUS-LIQUIDUS INTERFACE EXPERIMENTALLY DETERMINED UP TO 1000 atm*

Glen J. Schoessow

University of Florida, Gainesville, Florida

(Received 29 July 1968)

The triple-point pressure of four grades of graphite was determined to be 103 atm (absolute). The triple-point temperature varied from one grade to another with values ranging from 4183 ± 10 to $4299 \pm 25^\circ\text{K}$. The solidus-liquidus temperature measured for one grade increased with increasing pressure from 4247°K at 103 atm to 4306°K at 1000 atm.

The theoretical development of the graphite (carbon) phase diagram is receiving serious attention by this author and others; but until the theoretical results are more fruitful, the need for accurate experimental data is urgent.

The rapidly expanding use of graphite as a structural and ablative material for extreme high-temperature applications such as re-entry vehicles, supersonic-airplane leading edges, nuclear-rocket reactor and power reactor cores, etc., is making it essential to have accurate pressure-temperature phase-diagram data up to 1000 atm.

Graphite pressure-temperature phase-diagram research is made difficult by the normally non-compatible requirements of simultaneously maintaining high pressure and temperature for a test specimen. Investigators seeking experimental data on the graphite melting temperature are faced with many difficulties. Several approaches have been tried by Bassett,¹ Jones,² Noda,³ Bun-

dy,⁴ and Fateeva⁵ in order to maintain the desired environment and to accurately measure the melting temperature.

A test specimen large enough to make its own crucible provided the unique feature which allowed this work to achieve accurate results. The 11.5-mm-diam specimen was melted at the axial center line by electrical resistance heating, but remained solid at the outside surface at the time the melt temperature was achieved. A radial hole to the melt location provided an almost ideal blackbody cavity for the optical readings, thus eliminating the usual emissivity correction problem. A blackbody-calibrated monochromatic pyrometer was used for all temperature measurements. This pyrometer was calibrated by the National Bureau of Standards. Additional checks of the calibration were performed on the actual experimental setup by measuring the melting point of gold, molybdenum, and tungsten. The results of these tests verified the accuracy